J. Math. Biol. (2011) 62:453–478
DOI 10.1007/s00285-010-0343-y

Mathematical Biology

Control design for sustained oscillation in a two-gene regulatory network

Roderick Edwards · Sehjeong Kim · P. van den Driessche

Received: 12 February 2009 / Revised: 28 January 2010 / Published online: 27 April 2010

Abstract Control strategies for gene regulatory networks have begun to be explored, both experimentally and theoretically, with implications for control of disease as well as for synthetic biology. Recent work has focussed on controls designed to achieve desired stationary states. Another useful objective, however, is the initiation of sustained oscillations in systems where oscillations are normally damped, or even not present. Alternatively, it may be desired to suppress (by damping) oscillations that naturally occur in an uncontrolled network. Here we address these questions in the context of piecewise-affine models of gene regulatory networks with affine controls that match the qualitative nature of the model. In the case of two genes with a single relevant protein concentration threshold per gene, we find that control of production terms (constant control) is effective in generating or suppressing sustained oscillations, while control of decay terms (linear control) is not effective. We derive an easily calculated condition to determine an effective constant control. As an example, we apply our analysis to a model of the carbon response network in *Escherichia coli*, reduced to the two genes that are essential in understanding its behavior.

Keywords Gene regulatory networks · Piecewise-affine systems · Feedback control · Oscillations

Mathematics Subject Classification (2000) 92B05 · 34C25 · 34H05

R. Edwards (✉) · S. Kim · P. van den Driessche
Department of Mathematics and Statistics, University of Victoria, PO BOX 3060, STN CSC, Victoria, BC, Canada
e-mail: edwards@uvic.ca

S. Kim
e-mail: sjkim@uvic.ca

P. van den Driessche
e-mail: pvdd@uvic.ca

1 Introduction

Advances in the technology of measuring gene expression have made the experimental study of gene regulation increasingly feasible. This in turn has made it increasingly necessary to have mathematical tools for the analysis and understanding of the dynamical behavior of gene regulatory networks. It is most often the case, however, that precise detailed models are still not feasible, since even when the relevant transcription factors for a given gene and their mode of regulation are known, parameter values such as decay rates and production rates are usually not known with any precision. One approach to the study of dynamical behavior of networks in these circumstances is to use qualitative models that capture the essential features of regulatory interactions without requiring knowledge of exact parameters. Many of the interactions in gene networks are strongly switching, so we use piecewise-linear differential equations, as pioneered by Glass (1975) and others Casey et al. (2006), Edwards (2000), Edwards et al. (2001), Farcot (2006), Gouzé and Sari (2003), Mestl et al. (1995), Plahte and Kjøglum (2005). With this approximation, the interactions depend only on whether each transcription factor is above or below some threshold.

In addition to mapping out gene network interactions that exist naturally, another experimental objective is to be able to control the behavior of regulatory networks, and even to design new ones. The control problem is certainly important in the long-term goal of repairing gene regulatory systems that have gone awry, as for example in cancer. Control of network behavior may also be useful as a means of perturbing the normal behavior of harmful organisms, such as *E. coli*. Construction of gene networks in synthetic biology requires techniques closely allied to those of control of naturally occurring networks; see for example Hasty et al. (2001), Kobayashi et al. (2004), Elowitz and Liebler (2000). For example, oscillatory networks have been engineered by transcriptional mechanisms (Elowitz and Liebler 2000) and processes that also involve post-transcriptional mechanisms (Tigges et al. 2009). Specific control techniques to determine or modify production and degradation rates have been described in the experimental literature. These include the introduction of additional activators or repressors, as is done in synthesizing networks as cited above; introduction of biochemicals, such as engineered RNA, that modify existing regulatory processes, typically by binding; and introduction of enzymes that control DNA supercoiling that in turn alters reactions rates; see for example Isaacs et al. (2004, 2006), Maxwell (1999).

In the context of piecewise-affine models, the control problem was introduced by Farcot and Gouzé (2008). They dealt primarily with the problem of using a control to generate or relocate equilibria in a network of two genes, for example, to create bistable switches. They took their control variable to be piecewise-affine in the same way as the network itself, so that the control may be active or not depending on the regulatory level of the two genes. Experimentally, this is a plausible scenario, since biochemically, a control may be effective only in the presence or absence of one or more of the network's transcription factors. An argument for this approach is made by Farcot and Gouzé (2008). For example, a specific transcription factor may need to be present to bind to an introduced biochemical to carry out a new regulatory function.

The ideas proposed by Farcot and Gouzé (2008) could be generalized to networks with more than two genes, but here we address the problem of control to produce (or destroy) oscillatory behavior. From a practical point of view, it may be desirable to destabilize a network that produces harmful effects when in some stable state by inducing oscillation, or alternatively to damp out an undesirable oscillation. The need to control oscillations is a type of problem that occurs widely in mathematical biology, from oscillations in populations or infection outbreaks to oscillations in blood cell production or neuronal activity (as, for example, in Parkinson's disease). Many of these situations come under the heading of 'dynamical disease', a term coined by Mackey and Glass (1977).

Thus, our objective in this study is to examine the means by which a piecewise-affine control can generate sustained oscillations in a network that normally damps out oscillations, or inversely, to damp out oscillations in a network where they are normally sustained. We restrict ourselves to feedback loops of just two genes, but it should be pointed out that oscillations in networks of more than two genes may depend essentially on a simple feedback loop between two components, so that the analysis of the two-gene situation may often be enough to explain the behavior of larger networks; see, for example, Guantes and Poyatos (2006, Synopsis). This is the case in the model we use for illustration, that of Ropers et al. (2006), for which Grognard et al. (2007) showed that a six-gene network can be reduced to two for understanding the key dynamical issues. Like Farcot and Gouzé (2008), we consider piecewise-affine controls whose thresholds are those of network variables, and that modify production rates and decay rates.

We find that the constant control part manipulating the production term is effective in generating periodic orbits and has considerable flexibility in how it can be implemented. From a mathematical point of view, the essential idea is to increase a particular ratio of production parameters above a critical value. However, we find that the linear control part modifying the decay term does not contribute to producing a periodic orbit. This difference is itself an interesting result. The simple condition for the creation of a periodic orbit in our constant control design is also applicable in reverse (i.e., by decreasing the same ratio of parameters) as a condition for the destruction of a periodic orbit.

The paper is organized as follows. We introduce notation and describe the piecewise-affine model in Sect. 2. In Sect. 3, the condition for a periodic orbit in a two- dimensional gene regulatory network is provided in the situation where cycling among the network states is already possible, but oscillations are normally damped. In Sect. 4, the control scheme mentioned above is developed. In Sect. 5, we illustrate the procedure by applying the constant control scheme to a specific model, the *E. coli* network of Ropers et al. (2006). Finally, in Sect. 6, we discuss our results and their implications, and suggest possible future research questions.

2 Piecewise-affine gene regulatory networks

Suppose that there are n genes and each gene has $m_i - 1$ positive finite thresholds for $i = 1, \ldots, n$. Then, a piecewise-affine gene regulatory network that is modeled by differential equations can be written as

$$\dot{x}_i = -\gamma_i x_i + \gamma_i F_i(\tilde{x}_1, \ldots, \tilde{x}_n), \tag{1}$$

where $x_i \geq 0$ is the concentration level of the protein product of the ith gene, $\gamma_i > 0$ is the decay rate, and $\gamma_i F_i(\tilde{x}_1, \ldots, \tilde{x}_n) \geq 0$ is the production term, which is determined by $\tilde{x}_i$ for $i = 1, \ldots, n$; see, for example, Edwards (2000), Farcot and Gouzé (2008), Mestl et al. (1995) and the references therein. The argument $\tilde{x}_i$ is defined by

$$\tilde{x}_i = \sum_{j=1}^{m_i} a_i^j s^+(x_i, \theta_i^{j-1}) s^-(x_i, \theta_i^j) \tag{2}$$

where $0 < \theta_i^1 < \cdots < \theta_i^{m_i - 1} < \infty$ are thresholds of the ith gene with $\theta_i^0 = 0$ and $\theta_i^{m_i} = \infty$, $a_i^1, \ldots, a_i^{m_i}$ are distinct non-negative integers, and

$$s^+(x_\ell, \theta_\ell) = \begin{cases} 1 & \text{if } x_\ell > \theta_\ell \\ \\ 0 & \text{if } x_\ell < \theta_\ell \end{cases} \tag{3}$$

with $s^-(x_\ell, \theta_\ell) = 1 - s^+(x_\ell, \theta_\ell)$. In practice, $\theta_i^{m_i} = \Theta_i$, a finite upper bound on the protein concentration and $m_i - 1$ counts the number of positive thresholds not including Θ_i. Setting $\theta_i^{m_i} = \infty$ makes no difference dynamically.

The thresholds divide $\mathcal{R}^n$ into $\prod_{i=1}^n m_i$ rectangular regions D_k that are called *boxes* and defined by

$$D_k = (\theta_1^{j_1 - 1}, \theta_1^{j_1}) \times \cdots \times (\theta_n^{j_n - 1}, \theta_n^{j_n}), \tag{4}$$

where $k = 1, \ldots, \prod_{i=1}^n m_i$, $j_i = 1, \ldots, m_i$, for $i = 1, \ldots, n$. Then, in D_k (1) becomes

$$\dot{x}_i = -\gamma_i x_i + \gamma_i F_i(D_k), \tag{5}$$

where $F_i(D_k) = F_i(\tilde{x}_1, \ldots, \tilde{x}_n)|_{D_k}$ is evaluated via $\tilde{x}_i \in \{a_i^1, \ldots, a_i^{m_i}\}$. Then, $(F_1(D_k), \ldots, F_n(D_k))$ is called the *focal point* of the box D_k. By the nature of (5), if the focal point of D_k appears in D_k, once the trajectory of (1) crosses one of the boundaries of D_k, it converges to the focal point. However, the focal point may not appear in its own box D_k. Trajectories always leave such a box (unless the focal point is on the boundary of D_k). In general, a trajectory may never encounter a box containing its own focal point, and may, for example, converge to a fixed point on a box boundary, or cycle through a sequence of boxes. For some network structures, a cycle might have a corresponding periodic orbit.

To observe the above case, we consider a two-dimensional gene regulatory network with one positive, finite threshold per gene ($m_i = 2$ for $i = 1, 2$), which is the main focus of this paper. The evolution of such a network is given by the piecewise-affine model from (1)

$$\begin{cases} \dot{x}_1 = -\gamma_1 x_1 + \gamma_1 F_1(\tilde{x}_1, \tilde{x}_2) \\ \\ \dot{x}_2 = -\gamma_2 x_2 + \gamma_2 F_2(\tilde{x}_1, \tilde{x}_2) \end{cases} \tag{6}$$

with the notation as in (1) and $\tilde{x}_i$ defined by (2) and (3). Thus,

$$\begin{aligned}\tilde{x}_i &= a_i^1 s^+(x_i, \theta_i^0) s^-(x_i, \theta_i^1) + a_i^2 s^+(x_i, \theta_i^1) s^-(x_i, \theta_i^2) \\ &= a_i^1 s^-(x_i, \theta_i^1) + a_i^2 s^+(x_i, \theta_i^1)\end{aligned} \tag{7}$$

since $\theta_i^0 = 0$ and $\theta_i^2 = \infty$ for $i = 1, 2$. In order to analyze the dynamics mathematically, the threshold values are translated to the origin by the change of variables $y_1 = x_1 - \theta_1^1$ and $y_2 = x_2 - \theta_2^1$. Then, (6) can be written as

$$\begin{cases} \dot{y}_1 = -\gamma_1 y_1 + \gamma_1 (F_1(\tilde{y}_1, \tilde{y}_2) - \theta_1^1) \\ \dot{y}_2 = -\gamma_2 y_2 + \gamma_2 (F_2(\tilde{y}_1, \tilde{y}_2) - \theta_2^1) \end{cases} \tag{8}$$

with

$$\tilde{y}_i = s^+(y_i, 0) \tag{9}$$

for $i = 1, 2$, where $\tilde{y}_i = (\tilde{x}_i - a_i^1)/(a_i^2 - a_i^1)$. Equation (9) means

$$\tilde{y}_i = \begin{cases} 1 & \text{if } y_i > 0 \\ 0 & \text{if } y_i < 0 \end{cases} \tag{10}$$

for $i = 1, 2$. Since each gene has one threshold, there are boxes which correspond to the four quadrants of the y_1 and y_2 plane. We name them as follows: 11, 01, 00, 10, which correspond to the first to the fourth quadrant, respectively, in the two-dimensional plane. Then, we denote the four focal points $(F_1(\tilde{y}_1, \tilde{y}_2) - \theta_1^1, F_2(\tilde{y}_1, \tilde{y}_2) - \theta_2^1)$ in the four orthants as (f_{ij}^1, f_{ij}^2) according to the values of $\tilde{y}_i$ for $i, j = 0, 1$. For example, in the 00-orthant, $(F_1(0, 0) - \theta_1^1, F_2(0, 0) - \theta_2^1)$ is denoted by (f_{00}^1, f_{00}^2) as the focal point of the 00-orthant. Thus, (8) can be written as

$$\begin{cases} \dot{y}_1 = -\gamma_1 y_1 + \gamma_1 f_{ij}^1 \\ \dot{y}_2 = -\gamma_2 y_2 + \gamma_2 f_{ij}^2 \end{cases} \tag{11}$$

where $y_1 \geq -\theta_1^1$, $y_2 \geq -\theta_2^1$, and $f_{ij}^1 \geq -\theta_i^1$, $f_{ij}^2 \geq -\theta_i^2$.

If the focal point of each orthant appears clockwise in its neighbor orthant, there is a cycle with the clockwise direction. For instance, the focal point (f_{11}^1, f_{11}^2) of the 11-orthant appears in the 10-orthant, thus $f_{11}^1 > 0$ and $f_{11}^2 < 0$. In the following section, we establish conditions under which the cycle indeed can have a periodic orbit.

3 Condition for a periodic orbit

Assume that the two-gene network model with unequal decay rates in the form (11) has a cycle with the clockwise direction. In this section, we calculate a Poincaré map along the cycle, which gives a condition for that cycle to have an associated periodic orbit. In order to do this, we show the one-dimensional Poincaré map is bounded, increasing and concave down. For this reason, we focus on the derivative of the point on the Poincaré map after the first loop starting from an initial point on a boundary of any orthant, and evaluate this derivative at zero. If the value is greater than 1, then we conclude that the geometrically constructed cycle of (11) has a periodic orbit. Mestl et al. (1995) worked on a two-gene regulatory network model with equal decay rates ($\gamma_1 = \gamma_2$). The following theorem generalizes the result of Mestl et al. (1995, Appendix) to unequal decay rates and states the result in terms of

$$\Gamma = \frac{f_{01}^2}{f_{01}^1}\frac{f_{00}^1}{f_{00}^2}\frac{f_{10}^2}{f_{10}^1}\frac{f_{11}^1}{f_{11}^2}. \tag{12}$$

Theorem 1 *Assume that the system* (11) *has a cycle as described above. The cycle has a periodic orbit if and only if*

$$\Gamma > 1. \tag{13}$$

Proof By calculations in the Appendix, the Poincaré map is bounded, increasing and concave down; see (61). From a consideration of the Poincaré map, (11) has a periodic orbit if and only if the Jacobian

$$\left.\frac{dy_k^{(4)}}{dy_k^{(0)}}\right|_{y_k^{(0)}=0} > 1 \quad \text{for } k = 1 \text{ or } 2, \tag{14}$$

where $y_k^{(0)}$ and $y_k^{(4)}$ are one component of the boundary points at which the trajectory of (11) enters the zeroth and fourth orthants as it completes one loop of the cycle. To calculate the derivative of the point on the Poincaré map after the first loop, we can start from any orthant and follow along the cycle. Note that $(y_1^{(\ell)}, y_2^{(\ell)})$ is the point on the boundary where a trajectory of (11) crosses into the (ℓ)th orthant where ℓ implies one of the orthants, 11, 10, 00, or 01.

Now,

$$\begin{aligned}\left.\frac{dy_2^{(4)}}{dy_2^{(0)}}\right|_{y_2^{(0)}=0} &= \left.\frac{dy_2^{(4)}}{dy_1^{(3)}}\right|_{y_1^{(3)}=0}\left.\frac{dy_1^{(3)}}{dy_2^{(2)}}\right|_{y_2^{(2)}=0}\left.\frac{dy_2^{(2)}}{dy_1^{(1)}}\right|_{y_1^{(1)}=0}\left.\frac{dy_1^{(1)}}{dy_2^{(0)}}\right|_{y_2^{(0)}=0}\\ &= -\frac{f_{01}^2}{f_{01}^1}\frac{\gamma_2}{\gamma_1}\left(\frac{f_{01}^1}{f_{01}^1 - y_1^{(3)}}\right)^{(\gamma_2/\gamma_1)+1}\Bigg|_{y_1^{(3)}=0}\end{aligned}$$

$$\times -\frac{f_{00}^1}{f_{00}^2}\frac{\gamma_1}{\gamma_2}\left(\frac{f_{00}^2}{f_{00}^2 - y_2^{(2)}}\right)^{(\gamma_1/\gamma_2)+1}\Bigg|_{y_2^{(2)}=0}$$
$$\times -\frac{f_{10}^2}{f_{10}^1}\frac{\gamma_2}{\gamma_1}\left(\frac{f_{10}^1}{f_{10}^1 - y_1^{(1)}}\right)^{(\gamma_2/\gamma_1)+1}\Bigg|_{y_1^{(1)}=0}$$
$$\times -\frac{f_{11}^1}{f_{11}^2}\frac{\gamma_1}{\gamma_2}\left(\frac{f_{11}^2}{f_{11}^2 - y_2^{(0)}}\right)^{(\gamma_1/\gamma_2)+1}\Bigg|_{y_2^{(0)}=0}, \tag{15}$$

where details of the computation of the individual four derivatives are given in the Appendix. Simplifying (15) gives

$$\left.\frac{dy_2^{(4)}}{dy_2^{(0)}}\right|_{y_2^{(0)}=0} = \frac{f_{01}^2}{f_{01}^1}\frac{f_{00}^1}{f_{00}^2}\frac{f_{10}^2}{f_{10}^1}\frac{f_{11}^1}{f_{11}^2} = \Gamma \tag{16}$$

with Γ as defined in (12). From the signs of the focal points, Γ is positive. By (14), there is a periodic orbit if and only if $\Gamma > 1$. □

Remark 1 This condition on Γ is, in fact, essentially the same as the condition found by Mestl et al. (1995, Appendix) for a two-gene network with equal decay rates. If $\Gamma \leq 1$, then under the assumption of a cycle, the trajectory converges to the origin.

Corollary 1 *If the system in* (11) *has no self-input, then* $\Gamma = 1$ *and hence there is no periodic orbit.*

Proof No self-input means that each focal point coordinate is independent of a sign change of the corresponding variable (Edwards 2000, Condition 3). In other words, for $\text{sgn}(y_1) : + \to -$ (or vice versa), $f_{10}^1 = f_{00}^1$ and $f_{01}^1 = f_{11}^1$, for $\text{sgn}(y_2) : + \to -$ (or vice versa), $f_{11}^2 = f_{10}^2$ and $f_{00}^2 = f_{01}^2$. Thus,

$$\Gamma = \frac{f_{01}^2}{f_{01}^1}\frac{f_{00}^1}{f_{00}^2}\frac{f_{10}^2}{f_{10}^1}\frac{f_{11}^1}{f_{11}^2} = 1. \tag{17}$$

The result follows from Theorem 1. □

In the next section, we discuss possible control designs to achieve $\Gamma > 1$.

4 Control design for a periodic orbit

In order to generate a periodic orbit by accomplishing $\Gamma > 1$ for (11), consider the piecewise-affine control input given by

$$U_{ij} = (\gamma_1(H_{ij}^1 y_1 + u_{ij}^1), \gamma_2(H_{ij}^2 y_2 + u_{ij}^2))^T, \tag{18}$$

with $u^k_{\min} \le u^k_{ij} \le u^k_{\max}$ where $u^k_{\min}$ and $u^k_{\max}$ are minimum and maximum values for the constant input values, and H^k_{ij} and u^k_{ij} are constants for $k = 1, 2$ but may vary with $i, j = 0, 1$, and therefore depend on $\tilde{y}$. Then, with the control (18), equation (11) becomes

$$\begin{cases} \dot{y}_1 = -\gamma_1(1 - H^1_{ij})y_1 + \gamma_1(f^1_{ij} + u^1_{ij}) \\ \dot{y}_2 = -\gamma_2(1 - H^2_{ij})y_2 + \gamma_2(f^2_{ij} + u^2_{ij}). \end{cases} \tag{19}$$

We show that in the affine control (18), the constant control input part may create a sustained oscillator, whereas the linear control input part does not affect Γ in (12). The following theorem states the ineffectiveness of the linear control input part.

Theorem 2 *Suppose that* (11) *has a cycle and let the control input* U_{ij} *be given by* (18). *Then,* Γ *in* (12) *is not affected by the linear control input part but only by the constant control input part.*

Proof Suppose that the ij-orthant is entered with $(y_1^{(\ell)}, y_2^{(\ell)}) = (0, y_2^{(\ell)})$ for some $\ell \in \{0, 1, 2, 3\}$. Solving (19) with this initial condition,

$$\begin{cases} y_1 = \dfrac{f^1_{ij} + u^1_{ij}}{1 - H^1_{ij}} + \left(y_1^{(\ell)} - \dfrac{f^1_{ij} + u^1_{ij}}{1 - H^1_{ij}} \right) e^{-\gamma_1 t(1 - H^1_{ij})} = \dfrac{f^1_{ij} + u^1_{ij}}{1 - H^1_{ij}} - \dfrac{f^1_{ij} + u^1_{ij}}{1 - H^1_{ij}} e^{-\gamma_1 t(1 - H^1_{ij})} \\ y_2 = \dfrac{f^2_{ij} + u^2_{ij}}{1 - H^2_{ij}} + \left(y_2^{(\ell)} - \dfrac{f^2_{ij} + u^2_{ij}}{1 - H^2_{ij}} \right) e^{-\gamma_2 t(1 - H^2_{ij})}. \end{cases} \tag{20}$$

When the trajectory in (20) crosses the boundary into the ik-orthant, $y_2^{(\ell+1)} = 0$ and hence

$$e^{-\gamma_2 t(1 - H^2_{ij})} = \frac{(f^2_{ij} + u^2_{ij})/(1 - H^2_{ij})}{(f^2_{ij} + u^2_{ij})/(1 - H^2_{ij}) - y_2^{(\ell)}}. \tag{21}$$

Also,

$$e^{-\gamma_1 t(1 - H^1_{ij})} = \left(\frac{(f^2_{ij} + u^2_{ij})/(1 - H^2_{ij})}{(f^2_{ij} + u^2_{ij})/(1 - H^2_{ij}) - y_2^{(\ell)}} \right)^{\frac{\gamma_1(1 - H^1_{ij})}{\gamma_2(1 - H^2_{ij})}}, \tag{22}$$

so

$$y_1^{(\ell+1)} = \frac{f^1_{ij} + u^1_{ij}}{1 - H^1_{ij}} - \frac{f^1_{ij} + u^1_{ij}}{1 - H^1_{ij}} \left(\frac{(f^2_{ij} + u^2_{ij})/(1 - H^2_{ij})}{(f^2_{ij} + u^2_{ij})/(1 - H^2_{ij}) - y_2^{(\ell)}} \right)^{\frac{\gamma_1(1 - H^1_{ij})}{\gamma_2(1 - H^2_{ij})}}. \tag{23}$$

Thus,

$$\left.\frac{dy_1^{(\ell+1)}}{dy_2^{(\ell)}}\right|_{y_2^{(\ell)}=0} = -\frac{(f_{ij}^1+u_{ij}^1)/(1-H_{ij}^1)}{(f_{ij}^2+u_{ij}^2)/(1-H_{ij}^2)}\frac{\gamma_1(1-H_{ij}^1)}{\gamma_2(1-H_{ij}^2)}$$
$$\times\left.\left(\frac{(f_{ij}^2+u_{ij}^2)/(1-H_{ij}^2)}{(f_{ij}^2+u_{ij}^2)/(1-H_{ij}^2)-y_2^{(\ell)}}\right)^{\frac{\gamma_1(1-H_{ij}^1)}{\gamma_2(1-H_{ij}^2)}+1}\right|_{y_2^{(\ell)}=0}$$
$$= -\frac{f_{ij}^1+u_{ij}^1}{f_{ij}^2+u_{ij}^2}\frac{\gamma_1}{\gamma_2}, \tag{24}$$

which shows that the linear control gains H_{ij}^1 and H_{ij}^2 vanish in Γ in Theorem 1. Therefore, if the original Γ is not greater than 1, the linear control input part in (18) is not effective in generating a periodic orbit. □

Because of the result of Theorem 2, we now consider the possibility of sustained oscillators for system (11) under a constant control given by

$$U_{ij} = (\gamma_1 u_{ij}^1, \gamma_2 u_{ij}^2)^T, \tag{25}$$

where u_{ij}^k is a constant for $k = 1, 2$ and $i, j = 0, 1$. The control input values for u_{ij}^k are restricted so that the focal points remain in their original orthants; see Theorem 3 below. With this constant control, (19) can be written as

$$\begin{cases} \dot{y}_1 = -\gamma_1 y_1 + \gamma_1(f_{ij}^1 + u_{ij}^1) \\ \dot{y}_2 = -\gamma_2 y_2 + \gamma_2(f_{ij}^2 + u_{ij}^2). \end{cases} \tag{26}$$

The following theorems state the crucial control synthesis with given constant control.

Theorem 3 *Suppose that* (11) *has a cycle with* $\Gamma < 1$ *and let* u_{ij}^k *be constant in* (26). *Assume that* u_{ij}^k *is chosen such that for* $i, j = 0, 1$ *and* $k = 1, 2$ $sgn(f_{ij}^k + u_{ij}^k) = sgn(f_{ij}^k)$ *and either*

(i) *at least one of* $|f_{ij}^k + u_{ij}^k|$ *satisfies* $|f_{ij}^k + u_{ij}^k| < |f_{ij}^k|$ *with* $|f_{ij}^k + u_{ij}^k|$ *sufficiently small (but* $\neq 0$*) where* f_{ij}^k *is in the denominator of* Γ, *or*

(ii) *at least one of* $|f_{ij}^k + u_{ij}^k|$ *is sufficiently large where* f_{ij}^k *is in the numerator of* Γ.

Then, the constant control induces the cycle of (26) *to have a periodic orbit.*

Proof Note that the condition $\text{sgn}(f_{ij}^k + u_{ij}^k) = \text{sgn}(f_{ij}^k)$ for $i, j = 0, 1$ and $k = 1, 2$ in the assumption of Theorem 3 is necessary to preserve the cycle of the original uncontrolled system (11) by not moving focal points out of their original orthants. Suppose

that the ij-orthant is entered with $(y_1^{(\ell)}, y_2^{(\ell)}) = (0, y_2^{(\ell)})$ for some $\ell \in \{0, 1, 2, 3\}$. Then, from the proof of Theorem 2 with $H_{ij}^k = 0$, equation (24) holds. Therefore, as in the proof of Theorem 1, Γ in (12) becomes

$$\tilde{\Gamma} = \left(\frac{f_{01}^2 + u_{01}^2}{f_{01}^1 + u_{01}^1}\right)\left(\frac{f_{00}^1 + u_{00}^1}{f_{00}^2 + u_{00}^2}\right)\left(\frac{f_{10}^2 + u_{10}^2}{f_{10}^1 + u_{10}^1}\right)\left(\frac{f_{11}^1 + u_{11}^1}{f_{11}^2 + u_{11}^2}\right). \tag{27}$$

By the assumptions,

$$0 < (f_{01}^1 + u_{01}^1)(f_{00}^2 + u_{00}^2)(f_{10}^1 + u_{10}^1)(f_{11}^2 + u_{11}^2) \approx 0 << f_{01}^1 f_{00}^2 f_{10}^1 f_{11}^2,$$

or

$$(f_{01}^2 + u_{01}^2)(f_{00}^1 + u_{00}^1)(f_{10}^2 + u_{10}^2)(f_{11}^1 + u_{11}^1) \geq f_{00}^1 f_{01}^2 f_{10}^2 f_{11}^1 > 0.$$

Thus, $\tilde{\Gamma} > 1$ and the results follows from Theorem 1. □

Remark 2 As the assumptions in Theorem 3 address, the control input values are chosen such that the focal point in each orthant remains in its original orthant. Thus, each orthant has a control input space accordingly. Let I_{ij}^k denote the interval for each coordinate of the control input values u_{ij}^k and $\mathcal{U}_{ij}$ denote the control input space for the ij-orthant for $i, j = 0, 1$ and $k = 1, 2$. Then, the control input space $\mathcal{U}_{ij}$ for the ij-orthant is obtained as

$$\mathcal{U}_{ij} = I_{ij}^1 \times I_{ij}^2, \tag{28}$$

with each $\mathcal{U}_{ij}$ given as follows.

Input Space	I_{ij}^1	I_{ij}^2
$\mathcal{U}_{11}$	$0 \leq u_{11}^1 \leq u_{\max}^1$	$0 \leq u_{11}^2 < -f_{11}^2$
$\mathcal{U}_{10}$	$0 \leq u_{10}^1 < -f_{10}^1$	$u_{\min}^2 \leq u_{10}^2 \leq 0$
$\mathcal{U}_{00}$	$u_{\min}^1 \leq u_{00}^1 \leq 0$	$-f_{00}^2 < u_{00}^2 \leq 0$
$\mathcal{U}_{01}$	$-f_{01}^1 < u_{01}^1 \leq 0$	$0 \leq u_{01}^2 \leq u_{\max}^2$,

(29)

where $u_{\min}^k < 0$ and $u_{\max}^k > 0$ are the minimum and maximum values for u_{ij}^k, and $f_{11}^2, f_{10}^1 < 0$ and $f_{00}^2, f_{01}^1 > 0$ are coordinates of the focal points.

Corollary 2 *To obtain a periodic orbit for (26), it is sufficient to take one u_{ij}^k non-zero.*

Proof Equation (27) with u_{10}^1 non-zero and the other $u_{ij}^k = 0$ for $k = 1, 2$ and $i, j = 0, 1$ can be written as

$$\begin{aligned}\tilde{\Gamma} &= \left(\frac{f_{01}^2}{f_{01}^1}\right)\left(\frac{f_{00}^1}{f_{00}^2}\right)\left(\frac{f_{10}^2}{f_{10}^1 + u_{10}^1}\right)\left(\frac{f_{11}^1}{f_{11}^2}\right) \\ &= \frac{\beta}{f_{10}^1 + u_{10}^1},\end{aligned} \tag{30}$$

where $\beta = \dfrac{f_{01}^2 f_{00}^1 f_{10}^2 f_{11}^1}{f_{01}^1 f_{00}^2 f_{11}^2} < 0$ and $f_{10}^1 < 0$. So, $u_{10}^1 > 0$ can be chosen such that $\mathrm{sgn}(f_{10}^1 + u_{10}^1) = \mathrm{sgn}(f_{10}^1)$ and

$$|\beta| > |f_{10}^1 + u_{10}^1|.$$

By this choice of u_{10}^1, it follows that $|f_{10}^1 + u_{10}^1| < |f_{10}^1|$ and

$$\tilde{\Gamma} = \frac{\beta}{f_{10}^1 + u_{10}^1} > 1.$$

Thus, the cycle of (26) with only one non-zero control input value designed above has a periodic orbit. □

Remark 3 In the case that there is no cycle, a constant control can also induce a periodic orbit. As an example, Fig. 1 shows a situation in which the 01-orthant's focal point resides in the 01-orthant. Hence, the left-hand side figure indicates that all trajectories tend to converge to the 01-orthant's focal point. However, after shifting f_{01}^1 to the 11-orthant by applying a proper constant control $u_{01}^1 > 0$ such that from (27)

$$\tilde{\Gamma} = \left(\frac{f_{01}^2}{f_{01}^1 + u_{01}^1}\right)\left(\frac{f_{00}^1}{f_{00}^2}\right)\left(\frac{f_{10}^2}{f_{10}^1}\right)\left(\frac{f_{11}^1}{f_{11}^2}\right) > 1, \tag{31}$$

provided that $f_{01}^1 + u_{01}^1 > 0$ but $|f_{01}^1 + u_{01}^1|$ is sufficiently small, a periodic orbit is created as the right-hand side in Fig. 1 illustrates. This creation of a periodic orbit can be generalized to similar situations in which moving focal points across boundaries creates a cycle.

Suppose, in the absence of control input, there is a periodic orbit so that oscillations are sustained. By interchanging the roles of numerator and denominator of $\tilde{\Gamma}$ in (27), a control can be constructed to damp oscillations.

Theorem 4 *Suppose that* (11) *has a periodic orbit* (*i.e.,* $\Gamma > 1$). *If* u_{ij}^k *is chosen to satisfy* $sgn(f_{ij}^k + u_{ij}^k) = sgn\, f_{ij}^k$ *and* $\tilde{\Gamma} \leq 1$, *then the periodic orbit is destroyed by a constant control.*

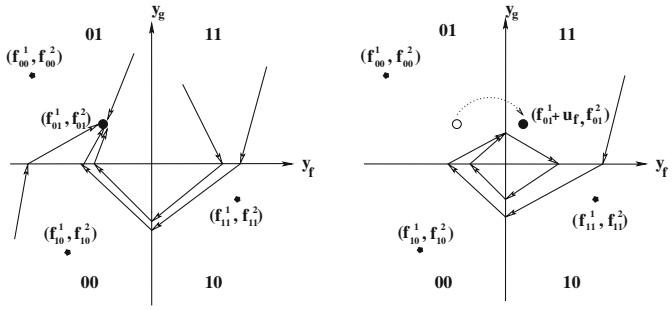

Fig. 1 The 01-orthant contains its own focal point hence the system does not have a cycle. By applying a proper control input value u_{01}^1 that shifts f_{01}^1 to the 11-orthant, a periodic orbit can be created

As shown in Theorem 3, only one non-zero value in the constant control input in (30) is required to change the original Γ in (12) to become greater than 1 to generate sustained oscillation. This control manipulation is relatively easy to apply experimentally since it only requires application to one gene. Although the linear control input part in Theorem 2 is applied to all genes and in all orthants, the linear control input part does not alter the value of the original Γ. Thus, in order to create sustained oscillation in a two-gene piecewise-affine network, control of decay rates is not effective whereas control of production terms can be effective and experimentally feasible.

5 Application: Carbon response of *E. coli*

As an application, we consider a model developed by Ropers et al. (2006) describing the carbon starvation response of *E. coli*. While nutrients are available, *E. coli* cells grow exponentially in a state called the *exponential phase*. However, in a nutrient-depleted environment the bacteria slows its growth and enters a state called the *stationary phase*. This radical switch from the exponential growth to the stationary level in *E. coli* explains how it can survive under conditions of carbon starvation over prolonged periods of time.

The transition from exponential phase to stationary phase is managed by a complex genetic regulatory network; see Grognard et al. (2007, Fig. 7). In the *E. coli* network of Ropers et al. (2006), there are six genes that are crucial in the carbon starvation response. The network includes genes encoding proteins with activity depending on the transduction of the carbon starvation signal (the global regulator *crp* and the adenylate cyclase *cya*), genes involved in the metabolism (the global regulator *fis*), cellular growth (the *rrn* genes coding for stable RNAs), and DNA supercoiling, an important modulator of gene expression (the topoisomerase *topA* and the gyrase *gyrAB*).

In the following section, we use the reduced *E. coli* model by Grognard et al. (2007). Ropers et al. (2006) reported that the transition from the presence of carbon sources to carbon starvation has been well studied analytically and experimentally, however, the reverse transition still raises questions. Grognard et al. (2007) indicated a qualitative damped oscillation in the reverse transition from stationary phase to exponential growth. By applying Theorem 1, we confirm that the oscillation is not sustained

oscillation, i.e., not a periodic orbit. In addition, by using the control scheme proposed in Theorem 3, we show that constant control of production terms can induce sustained oscillation.

5.1 Reduced model of the carbon response network

In the *E. coli* model of Ropers et al. (2006), a piecewise-affine model is used and is supplemented with parameter inequality constraints. Their final model consists of six state variables, one variable for the concentration of each of the six genes $((x_c, x_y, x_f, x_g, x_t, x_r)$ for (*crp, cya, fis, gyrAB, topA, rrn*)), and one carbon source indicator u_s as an input variable such that $u_s = 0$ in the presence of carbon sources and $u_s = 1$ in the absence of carbon sources. Inequality constraints on the threshold concentrations and parameters determine the location of the focal points.

A detailed qualitative simulation of the six-dimensional model system can be found in Ropers et al. (2006). Since not all variables in the model are important in contributing to the dynamics, Grognard et al. (2007) suggested a series of variable reductions so that x_c, x_y, x_r can be removed from the analysis. They obtained the following reduced model that is valid after some finite time:

$$\begin{cases} \dot{x_f} = (\kappa_f^1 + \kappa_f^2 s^+(x_g, \theta_g^1))s^-(u_s, \theta_s)s^-(x_f, \theta_f^5) - \gamma_f x_f \\ \dot{x}_g = \kappa_g(1 - s^+(x_g, \theta_g^2)s^-(x_t, \theta_t^1))s^-(x_f, \theta_f^4) - \gamma_g x_g \\ \dot{x}_t = \kappa_t s^+(x_g, \theta_g^2)s^-(x_t, \theta_t^1)s^+(x_f, \theta_f^4) - \gamma_t x_t. \end{cases} \tag{32}$$

Here x_f, x_g, and $x_t \geq 0$, the parameters and threshold values satisfy the following constraints:

$$\begin{cases} 0 < \theta_f^1 < \theta_f^2 < \theta_f^3 < \theta_f^4 < \theta_f^5 < \max_f, \quad \theta_f^1 < \frac{\kappa_f^1}{\gamma_f} < \theta_f^2, \quad \theta_f^5 < \frac{(\kappa_f^1 + \kappa_f^2)}{\gamma_f} < \max_f \\ 0 < \theta_g^1 < \theta_g^2 < \max_g, \quad \theta_g^2 < \frac{\kappa_g}{\gamma_g} < \max_g \\ 0 < \theta_t^1 < \theta_t^2 < \max_t, \quad \theta_t^2 < \frac{\kappa_t}{\gamma_t} < \max_t, \\ 0 < \theta_s < 1, \end{cases} \tag{33}$$

and

$$s^+(x_\ell, \theta_\ell) = \begin{cases} 1 \text{ if } x_\ell > \theta_\ell \\ 0 \text{ if } x_\ell < \theta_\ell \end{cases}$$

with $s^-(x_\ell, \theta_\ell) = 1 - s^+(x_\ell, \theta_\ell)$.

5.2 Control synthesis in the presence of a carbon source

Since x_t can be shown to be less than θ_t^1, the equation for x_t can be eliminated to give a two-dimensional system. In the presence of a carbon source, the carbon source indicator $u_s = 0$ in (32), and Grognard et al. (2007) showed that the model in (32) can be even reduced further to

$$\begin{cases} \dot{x_f} = (\kappa_f^1 + \kappa_f^2 s^+(x_g, \theta_g^1))s^-(x_f, \theta_f^5) - \gamma_f x_f \\ \dot{x}_g = \kappa_g s^-(x_g, \theta_g^2)s^-(x_f, \theta_f^4) - \gamma_g x_g \end{cases} \tag{34}$$

with $x_f \geq 0, x_g \geq 0$, and the first two sets of inequalities in (33). This system has a sliding mode when x_f or x_g changes value at θ_f^5 or θ_g^2, respectively. The sliding mode happens along two hyperplanes $x_f = \theta_f^5$ and $x_g = \theta_g^2$ called black walls. In general, a trajectory is attracted to a black wall from both sides and slides along it; this is called a sliding motion. For more details about the sliding motion, see Filippov (1988, Chapter 1), Plahte and Kjøglum (2005), and Gouzé and Sari (2003). The model in (34) is a second order piecewise-affine system with two thresholds in each direction. Grognard et al. (2007) showed that there is a damped oscillation around the point (θ_f^4, θ_g^1). In addition, Grognard et al. (2007) provided simple observations showing that the two black walls are attractive and all solutions on the black walls slide to the end point (θ_f^4, θ_g^2) or (θ_f^5, θ_g^1) in finite time. To fit into the analysis of Sec. 3 and 4, we translate the point (θ_f^4, θ_g^1) to $(0, 0)$. So, we introduce new variables $y_f = x_f - \theta_f^4$ and $y_g = x_g - \theta_g^1$. Then, (34) can be written as

$$\begin{cases} \dot{y}_f = -\gamma_f(y_f + \theta_f^4) + (\kappa_f^1 + \kappa_f^2 s^+(y_g, 0))s^-(y_f, \theta_f^5 - \theta_f^4) \\ \dot{y}_g = -\gamma_g(y_g + \theta_g^1) + \kappa_g s^-(y_f, 0)s^-(y_g, \theta_g^2 - \theta_g^1). \end{cases} \tag{35}$$

Here, $y_f \geq -\theta_f^4$ and $y_g \geq -\theta_g^1$, and the black walls are $y_f = \theta_f^5 - \theta_f^4 > 0, y_g > 0$ and $y_g = \theta_g^2 - \theta_g^1 > 0, y_f < 0$.

Define a rectangular region $\mathcal{D}$ as

$$\mathcal{D} = \{(y_f, y_g) | -\theta_f^4 \leq y_f \leq \theta_f^5 - \theta_f^4 \quad \text{and} \quad -\theta_g^1 \leq y_g \leq \theta_g^2 - \theta_g^1\}, \tag{36}$$

where the two black walls form part of the boundary. Note that this region is invariant due to the attractiveness of the black walls and the sliding motion of a trajectory of (35) once it is attracted to the black walls; see Grognard et al. (2007). Once a trajectory of (35) hits either of the black walls, it is pushed into the region $\mathcal{D}$, and spirals toward to the origin that was previously (θ_f^5, θ_g^2) before the translation. Hence, a damped

oscillation occurs in the region $\mathcal{D}$. We now verify this phenomenon by the result in Sect. 3. Thus, we consider the system (35) inside region $\mathcal{D}$ given by

$$\begin{cases} \dot{y}_f = -\gamma_f(y_f + \theta_f^4) + (\kappa_f^1 + \kappa_f^2 s^+(y_g, 0)) \\ \dot{y}_g = -\gamma_g(y_g + \theta_g^1) + \kappa_g s^-(y_f, 0). \end{cases} \tag{37}$$

The names of orthants are the same as in Sec. 2, and system (37) is a special case of (8) with $\gamma_1 F_1 = \kappa_f^1 + \kappa_f^2 s^+(y_g, 0)$ and $\gamma_2 F_2 = \kappa_g s^-(y_f, 0)$. Then, the focal points in the $y_f y_g$-plane are as follows with the signs given by inequalities in (33).

Orthant	Focal point	Signs of focal point
11	$(f_{11}^1, f_{11}^2) = \left(\frac{\kappa_f^1 + \kappa_f^2 - \gamma_f\theta_f^4}{\gamma_f}, -\theta_g^1\right)$	$(+,-)$
10	$(f_{10}^1, f_{10}^2) = \left(\frac{\kappa_f^1 - \gamma_f\theta_f^4}{\gamma_f}, -\theta_g^1\right)$	$(-,-)$
00	$(f_{00}^1, f_{00}^2) = \left(\frac{\kappa_f^1 - \gamma_f\theta_f^4}{\gamma_f}, \frac{\kappa_g - \gamma_g\theta_g^1}{\gamma_g}\right)$	$(-,+)$
01	$(f_{01}^1, f_{01}^2) = \left(\frac{\kappa_f^1 + \kappa_f^2 - \gamma_f\theta_f^4}{\gamma_f}, \frac{\kappa_g - \gamma_g\theta_g^1}{\gamma_g}\right)$	$(+,+)$

(38)

Notice that $f_{00}^1 = f_{10}^1$, $f_{00}^2 = f_{01}^2$, $f_{01}^1 = f_{11}^1$, and $f_{11}^2 = f_{10}^2$ since (35) has no self-input.

The positions of the focal points in Fig. 2 show that there is a clockwise cycle even in the presence of the black walls. Then, recalling the definition of Γ in (12),

$$\begin{aligned} \Gamma &= \frac{f_{01}^2 f_{11}^1 f_{10}^2 f_{00}^1}{f_{11}^2 f_{01}^1 f_{10}^1 f_{00}^2} \\ &= \frac{\left(\frac{\kappa_f^1 + \kappa_f^2 - \gamma_f\theta_f^4}{\gamma_f}\right)\left(\frac{\kappa_g - \gamma_g\theta_g^1}{\gamma_g}\right)\left(-\theta_g^1\right)\left(\frac{\kappa_f^1 - \gamma_f\theta_f^4}{\gamma_f}\right)}{\left(-\theta_g^1\right)\left(\frac{\kappa_f^1 + \kappa_f^2 - \gamma_f\theta_f^4}{\gamma_f}\right)\left(\frac{\kappa_f^1 - \gamma_f\theta_f^4}{\gamma_f}\right)\left(\frac{\kappa_g - \gamma_g\theta_g^1}{\gamma_g}\right)} = 1. \end{aligned} \tag{39}$$

Therefore, by Corollary 1, the cycle of (37) does not have a periodic orbit. As briefly mentioned before, the black walls attract trajectories of (35). Once, a trajectory hits either of the black walls, it evolves along the black wall until it hits one of the orthant boundaries. This effect forces the trajectory to move into the region $\mathcal{D}$. Hence, the cycle in (37) will definitely converge to the origin even in the presence of the black walls.

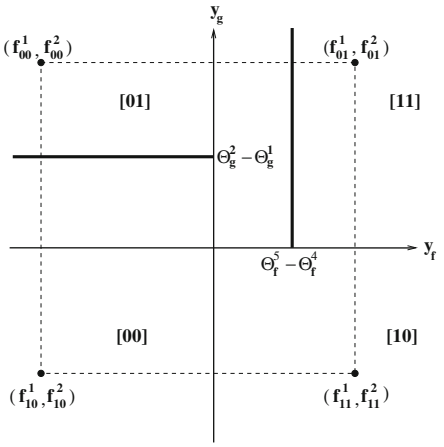

Fig. 2 Phase space of (35) showing four focal points and two black walls at $y_f = \theta_f^5 - \theta_f^4$ and $y_g = \theta_g^2 - \theta_g^1$. The dotted line is a reference to indicate that the *E. coli* model in (35) is a no self-input case

The best orthant in which to apply the constant control to the system (35) as described in Theorem 3 is the 10-orthant. The reason behind this is that a trajectory coming from the 11-orthant will not immediately enter an orthant with a black wall. In other words, any trajectory starting from either the 00, 01, or 11-orthant can hit one of two black walls, which tend to push the trajectory closer to the origin. Thus, any control in these orthants is not effective.

Applying the constant control to (35) gives

$$\begin{cases} \dot{y}_f = -\gamma_f(y_f + \theta_f^4) + (\kappa_f^1 + \kappa_f^2 s^+(y_g, 0))s^-(y_f, \theta_f^5 - \theta_f^4) \\ \qquad\quad +\gamma_f u_f s^+(y_f, 0)s^-(y_g, 0) \\ \dot{y}_g = -\gamma_g(y_g + \theta_g^1) + \kappa_g s^-(y_f, 0)s^-(y_g, \theta_g^2 - \theta_g^1) + \gamma_g u_g s^+(y_f, 0)s^-(y_g, 0), \end{cases} \tag{40}$$

where u_f and u_g are constants to be determined later. The factor $s^+(y_f, 0)s^-(y_g, 0)$ in (40) enables the constant control $U = (u_f, u_g)^T$ to work only in the 10-orthant. As shown in Corollary 2, u_g can be set to zero for a simpler control. In this case, the system is

$$\begin{cases} \dot{y}_f = -\gamma_f(y_f + \theta_f^4) + (\kappa_f^1 + \kappa_f^2 s^+(y_g, 0))s^-(y_f, \theta_f^5 - \theta_f^4) \\ \qquad\quad +\gamma_f u_f s^+(y_f, 0)s^-(y_g, 0) \\ \dot{y}_g = -\gamma_g(y_g + \theta_g^1) + \kappa_g s^-(y_f, 0)s^-(y_g, \theta_g^2 - \theta_g^1), \end{cases} \tag{41}$$

and only f_{10}^1 of the focal point in the 10-orthant is changed. For the region $\mathcal{D}$, the system is given by

$$\begin{cases} \dot{y}_f = -\gamma_f(y_f + \theta_f^4) + (\kappa_f^1 + \kappa_f^2 s^+(y_g, 0)) + \gamma_f u_f s^+(y_f, 0)s^-(y_g, 0) \\ \dot{y}_g = -\gamma_g(y_g + \theta_g^1) + \kappa_g s^-(y_f, 0). \end{cases} \tag{42}$$

From $\tilde{\Gamma}$ in (27) and because there is no self-input

$$\tilde{\Gamma} = \frac{f_{01}^2 f_{11}^1 f_{10}^2 f_{00}^1}{f_{11}^2 f_{01}^1 (f_{10}^1 + u_f) f_{00}^2} = \frac{f_{00}^1}{f_{10}^1 + u_f}. \tag{43}$$

Thus, $\tilde{\Gamma} > 1$ if and only if u_f satisfies the following:

(i) $\text{sgn}(f_{10}^1 + u_f) = \text{sgn}(f_{10}^1)$
(ii) $u_f > 0$

Conditions (i) and (ii) imply that this control choice pushes the original damped oscillation away from the origin. Hence, even with black walls, the control input $U = [u_f, 0]^T$ is effective. Note that a non-zero control input value for y_g as (ii) in Theorem 3 can be considered in order for (40) to have a periodic orbit. However, since f_{10}^2 is $-\theta_g^1$, which is already the lower bound for y_g, there is no room to pull f_{10}^2 down along the y_g axis to satisfy (ii) in Theorem 3.

We illustrate the above control result by simulations of the system (40) with parameter values as follows: $\gamma_f = 0.34, \gamma_g = 1, \theta_f^4 = 7.9, \theta_g^1 = 2.13, \kappa_f^1 = 0.7, \kappa_f^2 = 4, \kappa_g = 4.26, \theta_f^5 = 8.29, \theta_g^2 = 4$, thus, the black walls are at $y_f = \theta_f^5 - \theta_f^4 = 0.39$ and $y_g = \theta_g^2 - \theta_g^1 = 1.87$. Initial values are $(y_f^o, y_g^o) = (-3, 1.5)$.

Without control input, the focal points are to two decimal places

$$(f_{00}^1, f_{00}^2) = (-5.84, 2.13),\ (f_{01}^1, f_{01}^2) = (5.92, 2.13),$$
$$(f_{11}^1, f_{11}^2) = (5.92, -2.13),\ (f_{10}^1, f_{10}^2) = (-5.84, -2.13).$$

Without control, the trajectory of (35) with the initial values $(-3, 1.5)$ spirals in to the origin, as shown in Fig. 3.

Applying the constant control input value given by

$$U = (u_f, u_g)^T = (2.2, 0)^T$$

as in (41), f_{10}^1 is pushed closer to the y_g axis, and the trajectory generates a small periodic orbit in the region $\mathcal{D}$; see Fig. 4b.

As we can see in Figs. 3b and 4b, after the trajectory hits the black walls it is pushed into the region $\mathcal{D}$. In other words, the black walls work as barriers to a trajectory of (35) trapping it in $\mathcal{D}$. The attractiveness of the black walls is more clearly shown in Fig. 5b when a trajectory of (42) starts far from both of the black walls with the initial values $(-4, 3.6)$. Note that the scales in Fig. 5b are different from those in Figs. 3b and 4b. However, the constant control synthesis is indeed modifying the position of a targeted focal point, in our case, (f_{10}^1, f_{10}^2). It pushes or pulls one or all components of the targeted focal point near or along either the y_f or y_g axis. This constant controller drags down a trajectory entering the 10-orthant from the 11-orthant along the y_g axis, thus the trajectory evolves far from the origin after it enters the 10-orthant. Every time the trajectory comes back to the 10-orthant, no matter how close to the origin, it crosses into the 10-orthant from the 11-orthant and is pulled down away from the origin in the 10-orthant. This is how a periodic orbit is produced via the constant control. This control is very effective and easy to implement.

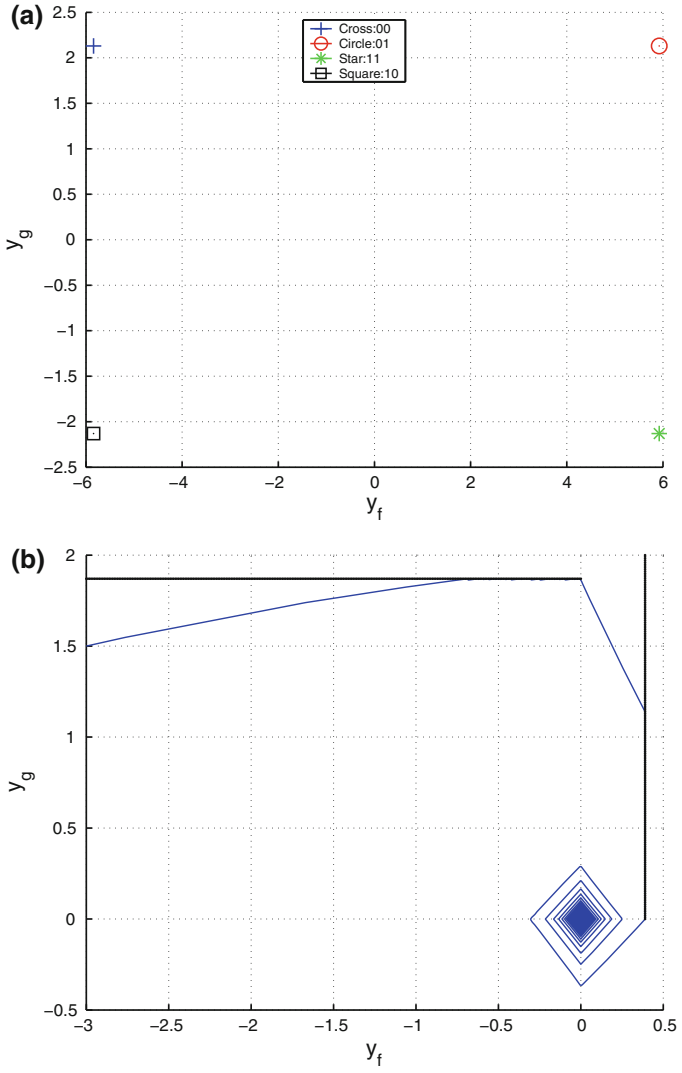

Fig. 3 Plots of (**a**) Focal points without any control input (**b**) y_f versus y_g with solutions converging to the origin. Parameters and initial values are as given in text with $f_{10}^1 = -5.84$. The *two dotted lines* indicate the black walls with $y_f = 0.39$ and $y_g = 1.87$

6 Discussion

In this study, we investigated the possible existence of sustained oscillations in a two-gene regulatory network (or sub-network). A piecewise-affine framework with unequal decay rates (11) was considered as a general model. Our main results deal with a situation where cycling through the system states is inherently possible (i.e., there is a cycle). First, we established a condition under which the cycle of (11) has

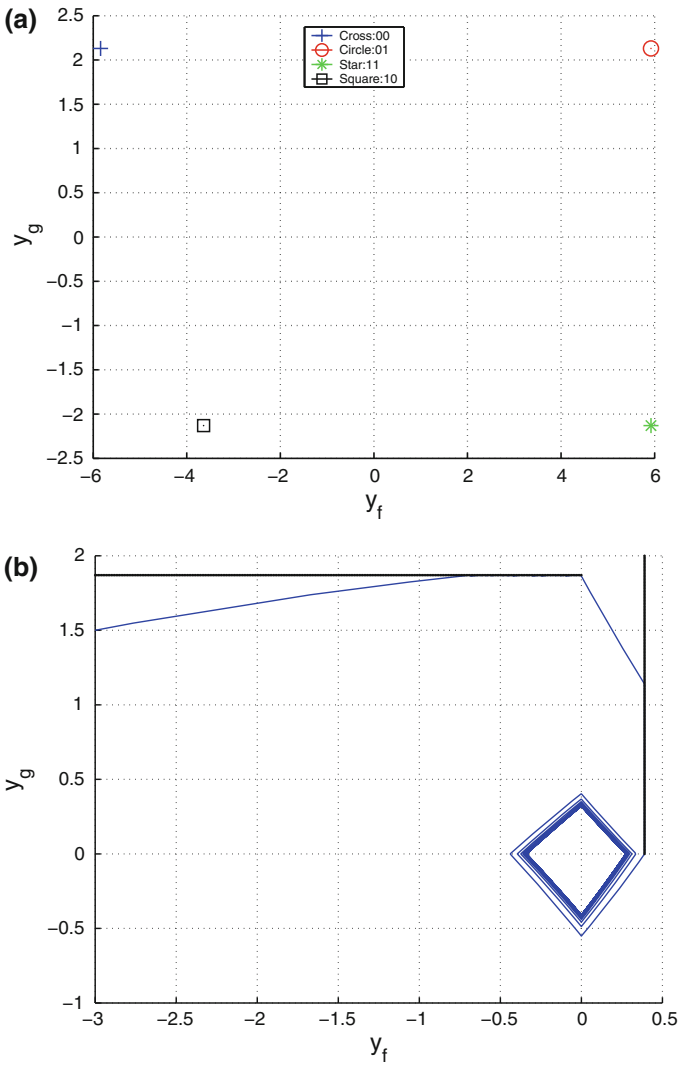

Fig. 4 Plots of (**a**) Focal points with one control input value $u_f = 2.2$ showing f_{10}^1 is pushed closer to the y_f axis (**b**) y_f versus y_g showing sustained oscillations. Parameters and initial values are as given in text with $f_{10}^1 = -3.64$. The *two dotted lines* indicate the black walls with $y_f = 0.39$ and $y_g = 1.87$

a periodic orbit. Second, in the case where the oscillations corresponding to the cycle are damped, we designed negative feedback control to destabilize the fixed point (11) at the origin. Our condition for a periodic orbit was obtained in terms of focal points (production parameters), which turned out to be the same as the condition of Mestl et al. (1995) in the context of equal decay rates. Our condition is easy to check as to whether or not a cycle has a periodic orbit. In addition, the reverse of the condition can be used as a tool to damp out a periodic orbit in a two-gene network.

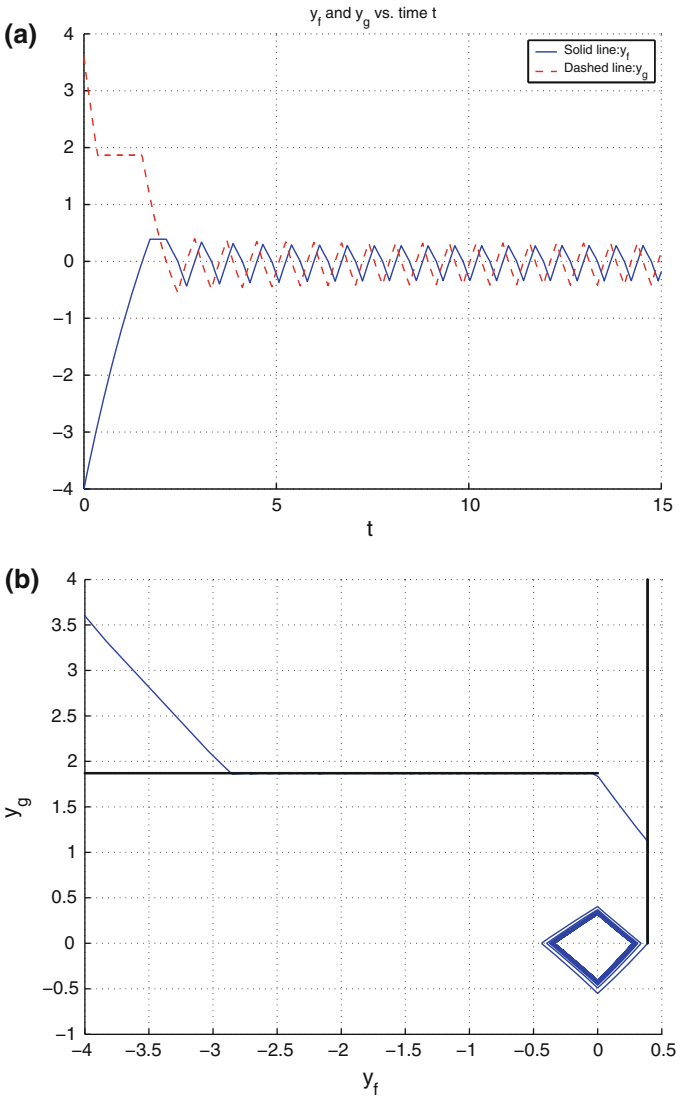

Fig. 5 The control input and parameters are as for Fig. 4, but new initial values $(-4, 3.6)$. **a** y_f and y_g versus time, respectively, and **b** y_g versus y_f. The *two dotted lines* indicate the black walls with $y_f = 0.39$ and $y_g = 1.87$. The periodic orbit is as in Fig. 4b

From the point of view of control design, a constant control for the production terms and a linear control for the decay terms in (11) prove to be quite different. In our piecewise-affine model, the constant control, which manipulates the production term in (11), is very effective in creating a periodic orbit even by moving just one of the focal points to satisfy the required condition for (11). On the other hand, the linear control, which manipulates the decay term in (11), is shown to be incapable of generating a periodic orbit. Although a linear control in a smooth model may be

capable of changing the system dynamics from sustained to damped oscillations (or *vice versa*), this controllability is sensitive to the gain of the sigmoidal functions; whereas a constant control is robust to variations of the gain. For example, Guantes and Poyatos (2006) showed two smooth models in which linear control is effective for low gain (quadratic terms in the production functions, i.e., cooperativity factor of 2). However, this controllability is lost if the cooperativity factor is sufficiently large. Our results indicate that in any such model linear controllability is lost in the large gain limit.

Furthermore, the constant control scheme may work even when there is no cycle. As shown in Sect. 4, the control scheme can change the position of a focal point targeted to another orthant in order to generate a periodic orbit by satisfying the condition (31) in the remark following Corollary 2.

We illustrated the constant control design by using the carbon starvation response model of Ropers et al. (2006) for *E. coli*, which has a cycle and two black walls. Even with the black walls that trap trajectories in a region near the origin (threshold intersection) and that force trajectories to converge to the origin in the absence of control input, the constant control scheme is nevertheless effective. In particular, the cycle acquires a periodic orbit when the focal point of the 10-orthant is pushed nearer to the y_g-axis. Since the equilibrium point in this carbon source case corresponds to a situation in which the *E. coli* population is growing, destabilization of the equilibrium point may have implications for the viability of the *E. coli* population.

The principle involved in the constant control scheme is mathematically quite simple. However, its simplicity makes it experimentally feasible. Control of more than one gene at a time is more difficult to accomplish experimentally, but our scheme only requires the control of a single gene. Our findings also suggest that, typically, there is flexibility in the choice of which gene to control, and there may be a number of choices that allow creation or suppression of oscillatory behavior. Although we concentrate on oscillation about a single pair of threshold values, our results are not incompatible with a situation in which each of the two genes has more than one threshold, as can be seen in the example of the *E. coli* model in (34). In networks with more than two genes, the existence of oscillation may depend essentially on the interaction of just two genes, in which case our analysis here applies. The six-dimensional *E. coli* model presented in Ropers et al. (2006) and analyzed here (Section 5) in two-dimensions, is an example of such a network. Our method of analyzing a two-dimensional system should be generalizable to cyclic behavior involving more than two genes, although it would be necessary to consider the eigenvalues of maps of dimensions greater than one, whereas Γ in (12) is the eigenvalue of a scalar map. Unless the decay rates γ_i are all equal, calculating these eigenvalues may be nontrivial.

Our theoretical results should help to guide further experimental work where the objective is to produce or suppress oscillations in gene networks.

Acknowledgments The research of RE and PvdD is partially supported by the Natural Science and Engineering Council (NSERC) of Canada Discovery grants. We thank Delphine Ropers and the anonymous reviewers for valuable comments.

Appendix

Calculations for the proof of Theorem 1:

In order to calculate the four derivatives $\left.\frac{dy_2^{(4)}}{dy_1^{(3)}}\right|_{y_1^{(3)}=0}$, $\left.\frac{dy_1^{(3)}}{dy_2^{(2)}}\right|_{y_2^{(2)}=0}$, $\left.\frac{dy_2^{(2)}}{dy_1^{(1)}}\right|_{y_1^{(1)}=0}$, and $\left.\frac{dy_1^{(1)}}{dy_2^{(0)}}\right|_{y_2^{(0)}=0}$, suppose that a trajectory of (11) crosses the boundary into the 11-orthant with the initial condition $(y_1^{(0)}, y_2^{(0)}) = (0, y_2^{(0)})$ with $y_2^{(0)} > 0$. Then,

$$\begin{cases} \dot{y}_1 = -\gamma_1 y_1 + \gamma_1 f_{11}^1 \\ \dot{y}_2 = -\gamma_2 y_2 + \gamma_2 f_{11}^2 \end{cases} \tag{44}$$

with $f_{11}^1 > 0$ and $f_{11}^2 < 0$. Solving (44) with the initial condition gives the trajectory

$$\begin{cases} y_1 = f_{11}^1 + (y_1^{(0)} - f_{11}^1)e^{-\gamma_1 t} = f_{11}^1 - f_{11}^1 e^{-\gamma_1 t} \\ y_2 = f_{11}^2 + (y_2^{(0)} - f_{11}^2)e^{-\gamma_2 t}. \end{cases} \tag{45}$$

When the trajectory crosses the boundary into the 10-orthant, $y_2^{(1)} = 0$ and hence

$$e^{-\gamma_2 t} = \frac{f_{11}^2}{f_{11}^2 - y_2^{(0)}} \Rightarrow e^{-\gamma_1 t} = \left(\frac{f_{11}^2}{f_{11}^2 - y_2^{(0)}}\right)^{\gamma_1/\gamma_2}. \tag{46}$$

Thus, when the trajectory of (44) crosses the boundary into the 10-orthant,

$$y_1^{(1)} = f_{11}^1 - f_{11}^1 \left(\frac{f_{11}^2}{f_{11}^2 - y_2^{(0)}}\right)^{\gamma_1/\gamma_2}. \tag{47}$$

Consider $dy_1^{(1)}/dy_2^{(0)}$ and $d^2y_1^{(1)}/dy_2^{(0)^2}$ as follows:

$$\begin{aligned} \frac{dy_1^{(1)}}{dy_2^{(0)}} &= -\frac{f_{11}^1}{f_{11}^2}\frac{\gamma_1}{\gamma_2}\left(\frac{f_{11}^2}{f_{11}^2 - y_2^{(0)}}\right)^{(\gamma_1/\gamma_2)+1} > 0, \\ \frac{d^2y_1^{(1)}}{dy_2^{(0)^2}} &= -f_{11}^1\frac{\gamma_1}{\gamma_2}\left(\frac{\gamma_1}{\gamma_2}+1\right)\left(\frac{f_{11}^2}{f_{11}^2 - y_2^{(0)}}\right)^{\gamma_1/\gamma_2}\frac{1}{(f_{11}^2 - y_2^{(0)})^2} < 0. \end{aligned} \tag{48}$$

This means that $y_1^{(1)}$ is concave down and increasing with respect to $y_2^{(0)}$. Note that $y_1^{(1)}$ is bounded such that $y_1^{(1)} \in [0, f_{11}^1)$ and the minimum value of $y_1^{(1)}$ as equal to zero and is obtained with $y_2^{(0)} = 0$.

When the trajectory of (44) enters the 10-orthant with $(y_1^{(1)}, 0)$, $y_1^{(1)} > 0$,

$$\begin{cases} \dot{y}_1 = -\gamma_1 y_1 + \gamma_1 f_{10}^1 \\ \dot{y}_2 = -\gamma_2 y_2 + \gamma_2 f_{10}^2 \end{cases} \tag{49}$$

with $f_{10}^1 < 0$ and $f_{10}^2 < 0$. By solving (49),

$$\begin{cases} y_1 = f_{10}^1 + (y_1^{(1)} - f_{10}^1)e^{-\gamma_1 t} \\ y_2 = f_{10}^2 + (y_2^{(0)} - f_{10}^2)e^{-\gamma_2 t} = f_{10}^2 - f_{10}^2 e^{-\gamma_2 t}. \end{cases} \tag{50}$$

When the trajectory in (49) hits the boundary of the 00-orthant, $y_1^{(2)} = 0$ and hence $e^{-\gamma_2 t} = \left(\frac{f_{10}^1}{f_{10}^1 - y_1^{(1)}}\right)^{\gamma_2/\gamma_1}$ giving

$$y_2^{(2)} = f_{10}^2 - f_{10}^2 \left(\frac{f_{10}^1}{f_{10}^1 - y_1^{(1)}}\right)^{\gamma_2/\gamma_1}. \tag{51}$$

Then, consider $dy_2^{(2)}/dy_1^{(1)}$ and $d^2y_2^{(2)}/dy_1^{(1)^2}$ as follows:

$$\begin{aligned} \frac{dy_2^{(2)}}{dy_1^{(1)}} &= -\frac{f_{10}^2}{f_{10}^1}\frac{\gamma_2}{\gamma_1}\left(\frac{f_{10}^1}{f_{10}^1 - y_1^{(1)}}\right)^{(\gamma_2/\gamma_1)+1} < 0, \\ \frac{d^2y_2^{(2)}}{dy_1^{(1)^2}} &= -f_{10}^2\frac{\gamma_2}{\gamma_1}\left(\frac{\gamma_2}{\gamma_1}+1\right)\left(\frac{f_{10}^1}{f_{10}^1 - y_1^{(1)}}\right)^{\gamma_2/\gamma_1}\frac{1}{(f_{10}^1 - y_1^{(1)})^2} > 0. \end{aligned} \tag{52}$$

This means that $y_2^{(2)}$ is concave up and decreasing with respect to $y_1^{(1)}$. In addition, since $y_1^{(1)}$ is bounded, $y_2^{(2)}$ is bounded. Since $y_1^{(1)}$ is bounded with respect to $y_2^{(0)}$, so is $y_2^{(2)}$. Note that

$$\begin{aligned} \frac{dy_2^{(2)}}{dy_2^{(0)}} &= \frac{dy_2^{(2)}}{dy_1^{(1)}}\frac{dy_1^{(1)}}{dy_2^{(0)}} < 0, \\ \frac{d^2y_2^{(2)}}{dy_2^{(0)^2}} &= \left(\frac{d^2y_2^{(2)}}{dy_1^{(1)^2}}\frac{dy_1^{(1)}}{dy_2^{(0)}}\right)\frac{dy_1^{(1)}}{dy_2^{(0)}} + \frac{dy_2^{(1)}}{dy_1^{(1)}}\frac{d^2y_1^{(1)}}{dy_2^{(0)^2}} > 0. \end{aligned} \tag{53}$$

When the trajectory of (49) enters the 00-orthant with $(0, y_2^{(2)})$, $y_2^{(2)} < 0$,

$$\begin{cases} \dot{y}_1 = -\gamma_1 y_1 + \gamma_1 f_{00}^1 \\ \dot{y}_2 = -\gamma_2 y_2 + \gamma_2 f_{00}^2 \end{cases} \tag{54}$$

with $f_{00}^1 < 0$ and $f_{00}^2 > 0$. When the trajectory of (54) hits the boundary into the 01-orthant, $y_2^{(3)} = 0$ and hence as in (47)

$$y_1^{(3)} = f_{00}^1 - f_{00}^1 \left(\frac{f_{00}^2}{f_{00}^2 - y_2^{(2)}} \right)^{\gamma_1/\gamma_2}. \tag{55}$$

Then, consider $dy_1^{(3)}/dy_2^{(2)}$ and $d^2y_1^{(3)}/dy_2^{(2)^2}$ as follows:

$$\begin{aligned} \frac{dy_1^{(3)}}{dy_2^{(2)}} &= -\frac{f_{00}^1}{f_{00}^2}\frac{\gamma_1}{\gamma_2}\left(\frac{f_{00}^2}{f_{00}^2 - y_2^{(2)}} \right)^{(\gamma_1/\gamma_2)+1} > 0, \\ \frac{d^2y_1^{(3)}}{dy_2^{(2)^2}} &= -f_{00}^2\frac{\gamma_1}{\gamma_2}\left(\frac{\gamma_1}{\gamma_2} + 1 \right)\left(\frac{f_{00}^2}{f_{00}^2 - y_2^{(2)}} \right)^{\gamma_1/\gamma_2} \frac{1}{(f_{00}^2 - y_2^{(2)})^2} > 0. \end{aligned} \tag{56}$$

This implies that $y_1^{(3)}$ is concave up and increasing with respect to $y_2^{(2)}$. By the same argument as above, $y_1^{(3)}$ is bounded with respect to $y_2^{(0)}$. Note that

$$\begin{aligned} \frac{dy_1^{(3)}}{dy_2^{(0)}} &= \frac{dy_1^{(3)}}{dy_2^{(2)}}\frac{dy_2^{(2)}}{dy_1^{(1)}}\frac{dy_1^{(1)}}{dy_2^{(0)}} < 0, \\ \frac{d^2y_1^{(3)}}{dy_2^{(0)^2}} &= \frac{d^2y_1^{(3)}}{dy_2^{(2)^2}}\left(\frac{dy_2^{(2)}}{dy_1^{(1)}}\frac{dy_1^{(1)}}{dy_2^{(0)}} \right)^2 + \frac{dy_1^{(3)}}{dy_2^{(2)}}\frac{d^2y_2^{(2)}}{dy_2^{(0)^2}} > 0. \end{aligned} \tag{57}$$

When the trajectory enters the 01-orthant with $(y_1^{(3)}, 0)$, $y_1^{(3)} < 0$,

$$\begin{cases} \dot{y}_1 = -\gamma_1 y_1 + \gamma_1 f_{01}^1 \\ \dot{y}_2 = -\gamma_2 y_2 + \gamma_2 f_{01}^2 \end{cases} \tag{58}$$

with $f_{01}^1 > 0$ and $f_{01}^2 > 0$. When the trajectory of (58) hits the boundary of the 11-orthant, $y_1^{(4)} = 0$ and hence as in (51)

$$y_2^{(4)} = f_{01}^2 - f_{01}^2 \left(\frac{f_{01}^1}{f_{01}^1 - y_1^{(3)}} \right)^{\gamma_2/\gamma_1}. \tag{59}$$

Then, consider $dy_2^{(4)}/dy_1^{(3)}$ and $d^2y_2^{(4)}/dy_1^{(3)^2}$ as follows:

$$\begin{aligned} \frac{dy_2^{(4)}}{dy_1^{(3)}} &= -\frac{f_{01}^2}{f_{01}^1}\frac{\gamma_2}{\gamma_1}\left(\frac{f_{01}^1}{f_{01}^1 - y_1^{(3)}} \right)^{(\gamma_2/\gamma_1)+1} < 0, \\ \frac{d^2y_2^{(4)}}{dy_1^{(3)^2}} &= -f_{01}^2\frac{\gamma_2}{\gamma_1}\left(\frac{\gamma_2}{\gamma_1} + 1 \right)\left(\frac{f_{01}^1}{f_{01}^1 - y_1^{(3)}} \right)^{\gamma_2/\gamma_1} \frac{1}{(f_{01}^1 - y_1^{(3)})^2} < 0. \end{aligned} \tag{60}$$

This means that $y_2^{(4)}$ is concave down and decreasing with respect to $y_1^{(3)}$. In addition, since $y_1^{(3)}$ is bounded by $y_2^{(0)}$, so is $y_2^{(4)}$.

Since one loop is completed by starting from the 11-orthant along with the geometrically constructed cycle of the sequence $11 \to 10 \to 00 \to 01$, we now need to consider $dy_2^{(4)}/dy_2^{(0)}$ and $d^2y_2^{(4)}/dy_2^{(0)^2}$ as follows:

$$\begin{aligned}
\frac{dy_2^{(4)}}{dy_2^{(0)}} &= \frac{dy_2^{(4)}}{dy_1^{(3)}}\frac{dy_1^{(3)}}{dy_2^{(2)}}\frac{dy_2^{(2)}}{dy_1^{(1)}}\frac{dy_1^{(1)}}{dy_2^{(0)}} > 0, \\
\frac{d^2y_2^{(4)}}{dy_2^{(0)^2}} &= \frac{d^2y_2^{(4)}}{dy_1^{(3)^2}}\left(\frac{dy_1^{(3)}}{dy_2^{(2)}}\frac{dy_2^{(2)}}{dy_1^{(1)}}\frac{dy_1^{(1)}}{dy_2^{(0)}}\right)^2 + \frac{dy_2^{(4)}}{dy_1^{(3)}}\frac{d^2y_1^{(3)}}{dy_2^{(0)^2}} < 0. \qquad (61)
\end{aligned}$$

Thus, $y_2^{(4)}$ is concave down, strictly increasing and bounded with respect to $y_2^{(0)}$. Note that $y_2^{(0)} = 0 \Rightarrow y_1^{(1)} = 0 \Rightarrow y_2^{(2)} = 0 \Rightarrow y_1^{(3)} = 0$.

References

Casey E, de Jong H, Gouzé J-L (2006) Piecewise-linear models of genetic regulatory netoworks: equilibria and their stability. J Math Biol 52:27–56

Edwards R (2000) Analysis of continuous-time switching networks. Phys D 146:165–199

Edwards R, Siegelmann HT, Aziza K, Glass L (2001) Symbolic dyanamics and computation in model gene networks. Chaos 11:160–169

Elowitz MB, Liebler S (2000) A synthetic oscillatory network of transcriptional regulators. Nature 403: 335–338

Farcot E (2006) Some geometric properties of piecewise affine biological network models. J Math Biol 52:373–418

Farcot E, Gouzé J-L (2008) A mathematical framework for the control of piecewise-affine models of gene networks. Automatica 44:2326–2332

Filippov AF (1988) Differential equations with discontinuous right-hand sides. Kluwer, Dordrecht

Glass L (1975) Combinatorial and topological methods in nonlinear chemical kinetics. J Chem Phys 63:1325–1335

Gouzé J-L, Sari T (2003) A class of piecewise linear differential equations arising in biological models. Dyn Syst 17:299–316

Grognard F, de Jong H, Gouzé J-L (2007) Piecewise-linear models of genetic regulatory networks: theory and example. In: Queinnec I et al (eds) Biology and control theory: current challenges. Lecture notes in control and information sciences (LNCIS), vol 357. Springer, Berlin, pp 137–159

Guantes R, Poyatos JF (2006) Dynamical principles of two-component genetic oscillators. PLoS Comput Biol 2:e30

Hasty J, Isaacs F, Dolnik M, McMillen D, Collins JJ (2001) Designer gene networks: towards fundamental cellular control. Chaos 11:207–220

Isaacs FJ, Dwyer DJ, Collins JJ (2006) RNA synthetic biology. Nat Biotech 24:545–554

Isaacs FJ, Dwyer DJ, Ding C, Pervouchine DD, Cantor CR, Collins JJ (2004) Engineered riboregulators enable post-transcriptional control of gene expression. Nat Biotechnol 22:841–847

Kobayashi H, Kærn M, Araki M, Chung K, Gardner TS, Cantor CR, Collins JJ (2004) Programmable cells: interfacing natural and engineered gene networks. Proc Natl Acad Sci 101:8414–8419

Mackey M, Glass L (1977) Oscillation and chaos in physiological control systems. Science 197:287–289

Maxwell A (1999) DNA gyrase as a drug target. Biochem Soc Trans 27:48–53

Mestl T, Plahte E, Omholt SW (1995) Periodic solutions in systems of piecewise-linear differential equations. Dyn Stabil Syst 10:179–193

Plahte E, Kjøglum S (2005) Analysis and generic properties of gene regulatory networks with graded response functions. Phys D 201:150–176

Ropers D, de Jong H, Page M, Schneider D, Geiselmann J (2006) Qualitative simulation of the carbon starvation response in *Escherichia coli*. BioSystems 84:124–152

Tigges M, Marquez-Lago TT, Stelling J, Fussenegger M (2009) A tunable synthetic mammalian oscillator. Nature 457:309–312